Crystal-Field and Covalency Effects in Uranates

An X-ray Spectroscopic Study

Butorin, Sergei M.; Kvashnina, Kristina O.; Smith, Anna L.; Popa, Karin; Martin, Philippe M.

DOI
10.1002/chem.201505091

Publication date
2016

Document Version
Accepted author manuscript

Published in
Chemistry: A European Journal

Crystal-field and covalency effects in uranates: x-ray spectroscopic study

Sergei M. Butorin,[*,†] Kristina O. Kvashnina,[‡,⊥] Anna L. Smith,[¶] Karin Popa,[§] and Philippe M. Martin[‖]

†*Department of Physics and Astronomy, Uppsala University, P. O. Box 516, SE-751 20 Uppsala, Sweden*
‡*European Synchrotron Radiation Facility, 6 rue Jules Horowitz, BP 220, 38043, Grenoble, France*
¶*TU Delft, Department of Radiation Science and Technology, Mekelweg 15, 2629 JB Delft, Netherlands*
§*European Commission, Joint Research Centre, Institute for Transuranium Elements, P.O. Box 2340, D-76125 Karlsruhe, Germany*
‖*CEA Marcoule, CEA, DEN, DTEC/SECA/LCC, F-30207 Bagnols-sur-Cze Cedex, France*
⊥*Helmholtz-Zentrum Dresden-Rossendorf (HZDR), Institute of Resource Ecology, P.O. Box 510119, 01314, Dresden, Germany*

Received May 19, 2016; E-mail: sergei.butorin@physics.uu.se

Abstract: The electronic structure of U(V) and U(VI) containing uranates $NaUO_3$ and Pb_3UO_6 was studied using an advanced technique, namely x-ray absorption spectroscopy (XAS) in the high-energy-resolution fluorescence-detection (HERFD) mode. Thanks to a significant reduction of the core-hole lifetime broadening, the crystal-field splittings of the $5f$ shell were probed directly in the HERFD-XAS spectra collected at the U $3d$ edge, which is not possible with conventional XAS. In addition, the charge-transfer satellites resulting from the U $5f-$O $2p$ hybridization were clearly resolved. The crystal-field parameters, $5f$ occupancy, and degree of covalency of the chemical bonding in these uranates were estimated using the Anderson impurity model by calculating the U $3d$ HERFD-XAS, conventional XAS, core-to-core (U $4f$-to-$3d$ transitions) resonant inelastic x-ray scattering (RIXS) and U $4f$ x-ray photoelectron spectra, respectively. The crystal field was found to be strong in these systems, while the $5f$ occupancy was determined to be 1.32 and 0.84 electrons in the ground state for $NaUO_3$ and Pb_3UO_6, respectively, thus indicating a significant covalent character for these compounds.

Uranates are systems of interest both from an applied and fundamental point of view. In case of an accident in a sodium-cooled and lead-cooled nuclear reactor, the coolant may come into contact with the fuel leading to the formation of sodium or lead uranates. A thorough knowledge of the structural, thermomechanical and thermodynamic properties of the uranate compounds is essential from safety prospectives. In particular, the oxidation state of the uranium cation is directly related to the oxyden potential threshold of formation, and is therefore a crucial parameter. From a fundamental point of view, uranates are of interest to researchers as perovskite-like systems which can contain uranium in different oxidation states, such as U(IV), U(V) and U(VI), with potentially strong crystal fields acting on the $5f$ shell.

In particular, $NaUO_3$ has attracted attention as solid with nominal U(V) but without a very complex chemical formula. This compound is one of the very few which was expected to contain only U(V) as opposed to a mixed valence state. The U(V) chemistry for solids is significantly less developed than that for U(IV) and U(VI) compounds.

Early x-ray photoelectron spectroscopy (XPS) measurements at the U $4f$ core levels of $NaUO_3$ did not confirm the U(V) state,[1] however, but rather suggested the presence of the U(IV)+U(VI) combination.[2] Such mixed valence state was not supported by the neutron diffraction experiments,[3,4] which found only one type of U atom in this compound with slightly distorted orthorhombic perovskite crystal structure. Based on the analysis of the x-ray absorption spectroscopy (XAS) data at the U L_3 edge of $NaUO_3$[5,6] and the energy shifts of the spectra, it was concluded that uranium is indeed in the U(V) state. Furthermore, the recent XPS measurements[7] at the U $4f$ core-levels of a $NaUO_3$ sample with etched and clean surface confirmed the presence of U(V) from the results of both the binding energy of the main U $4f$ XPS line and the energy difference between the main line and the satellite. However, the conclusions could still be questioned based on the argument that the energy shifts of the U L_3 spectra could also be caused by a redistribution of the U $6d$ density of states (DOS)[8–10] and not necessarily by a change in the chemical state of the uranium.

Recently, it was shown[11] that XAS measurements at the U $3d$ edge in the high energy resolution fluorescence detection (HERFD) mode could easily distinguish between U(IV), U(V) and U(VI) oxidation states thanks to a significant reduction in the core-hole lifetime broadening of the HERFD-XAS spectra. Applying the latter technique to $NaUO_3$ in the present work, we confirm that uranium is indeed in the U(V) state.

Furthermore, we show that thanks to the drastic improvement in resolution, it is now possible to probe the crystal-field strength and the crystal-field splittings in the U $5f$ shell directly from the HERFD-XAS spectra of uranates with U(V) and U(VI), and extract information on the degree of $5f$ hybridization with the ligand states and covalency of the chemical bonding from the analysis of the resolved U $5f-$O $2p$ charge-transfer satellites.

The measurements in the energy range of the U $3d$ x-ray absorption edge were performed at beamline ID26[12] of the European Synchrotron Radiation Facility in Grenoble. The incident energies were selected using the <111> reflection from a double Si-crystal monochromator. A rejection of higher harmonics was achieved by three Si mirrors at an angle of 3.5 mrad relative to the incident beam.

The XAS data were measured in the HERFD mode using the x-ray emission spectrometer.[13] The sample, analyzer crystal and photon detector (silicon drift diode) were arranged in a vertical Rowland geometry. The U HERFD spectra at the M_4 ($3d_{3/2} \rightarrow 5f_{5/2}, 7p$ transitions) edge were

obtained by recording the outgoing photons with an energy of ∼3337 eV as a function of the incident energy. This emission energy which corresponds to the maximum of the U $M\beta$ ($4f_{5/2} \rightarrow 3d_{3/2}$ transitions) x-ray emission line was selected using the <220> reflection of a single spherically bent Ge crystal analyzer (with 1m bending radius) aligned at 75° Bragg angle. The directions of the incident and emitted photons were 45° to the surface of the sample. The paths of the incident and emitted x-rays through air were minimized in order to avoid losses in intensity due to absorption. The spectral intensity was normalized to the incident flux. A combined (incident convoluted with emitted) energy resolution of 0.4 eV was obtained as determined by measuring the full width at half maximum (FWHM) of the elastic peak.

The $NaUO_3$ material was kindly provided by NRG (Nuclear Research and Consultancy Group, Petten, The Netherlands). In the case of the Pb_3UO_6 preparation, the starting chemicals were amorphous UO_3 (prepared in house from uranium dioxide) and lead(II) oxide (Sigma-Aldrich, 99.98% trace metal basis). Pure Pb_3UO_6 was obtained after 48 h of solid state reaction of stoichiometric admixtures at 873 K under air. The x-ray diffraction characterization did not reveal any secondary phases, and the refined cell parameters were found in good agreement with the reported values.[4,14] The $NaUO_3$ and Pb_3UO_6 samples were in the form of pellets. The UO_2 sintered pellet (theoretical density of 98%) was thermally treated for 24 h at 1700 °C under an Ar/5% H_2 atmosphere in order to assure its stoichiometry. X-ray diffraction results showed the fluorite type structure with a cell parameter corresponding to stoichiometric UO_2. For the HERFD-XAS measurements, the samples were encapsulated in double containment due to safety requirements for which the 8 μm Kapton film was used. No radiation damage of the samples was detected during the experiment.

The Anderson impurity model[15] (AIM) was used for the calculations which included the $5f$ and core ($3d$ or $4f$) states on a single actinide ion and a filled ligand $2p$ band. The calculations were performed in a manner described in Refs.[16–18]

To simulate a spectrum obtained in the HERFD-XAS mode, the resonant inelastic x-ray scattering (RIXS) map around the actinide $M\beta$ line was calculated using the Kramers-Heisenberg formula

$$I_{q_2,q_1}(\omega,\omega') = \sum_j \left| \sum_m \frac{\langle j|rC^{(1)}_{q_2}|m\rangle\langle m|rC^{(1)}_{q_1}|g\rangle}{E_g+\omega-E_m-i\Gamma_m/2} \right|^2 \times \frac{\Gamma_j/\pi}{(E_j+\omega'-E_g-\omega)^2+\Gamma_j^2}, \quad (1)$$

where $|g\rangle$, $|m\rangle$ and $|j\rangle$ are the ground, intermediate and final states of the spectroscopic process with energies E_g, E_m and E_j, respectively. ω and ω' are the energies of the incident and scattered/emitted photons with polarizations q_1 and q_2, respectively, and Γ_m and Γ_j are the lifetime broadenings of the intermediate and final states in terms of half width at half maximum (HWHM). Operators for optical dipole transitions (D) are expressed in terms of spherical tensor operators $C^{(1)}_q$ so that $q = 1, 0$, and -1 correspond to +helicity, linear, and −helicity polarizations.

The HERFD-XAS spectrum is described by a linear cut of such a RIXS map (see e.g. Ref.[11]) along the diagonal of the plane defined by the incident energy axis and energy transfer axis or parallel to the incident energy axis at a constant emitted energy (the energy of the $M\beta$ maximum in this case) in the plane of the emitted versus incident energies.

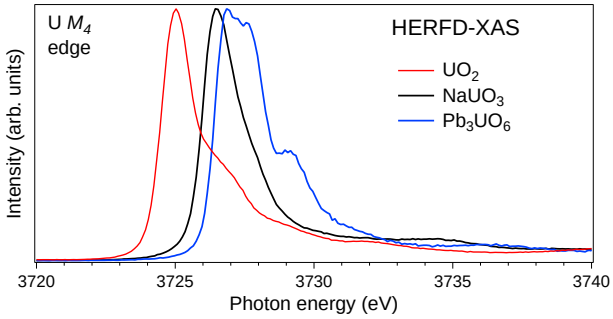

Figure 1. High resolution x-ray absorption spectra at the U M_4 edge of UO_2, $NaUO_3$ and Pb_3UO_6.

The conventional XAS and core-level XPS spectra were calculated using the following equations

$$I_{XAS}(\omega) = \sum_m |\langle m|D|g\rangle|^2 \frac{\Gamma_m/\pi}{(E_m-E_g-\omega)^2+\Gamma_m^2}. \quad (2)$$

and

$$I_{XPS}(E_B) = \sum_f |\langle f|a_c|g\rangle|^2 \frac{\Gamma_f/\pi}{(E_f-E_g-E_B)^2+\Gamma_f^2}. \quad (3)$$

where $|f\rangle$ is the XPS final state with energy E_f, E_B is the binding energy, and a_c is the annihilation operator of a core electron.

The required Slater integrals F^k, G^k and R^k,[19] spin-orbit coupling constants ζ and matrix elements were obtained with the TT-MULTIPLETS package which combines Cowan's atomic multiplet program[20] (based on the Hartree-Fock method with relativistic corrections) and Butler's point-group program,[21] which were modified by Thole,[22] as well as the charge-transfer program written by Thole and Ogasawara.

It should be pointed out that in such calculations it is difficult to reproduce accurately the absolute energies (the difference with the experiment is usually in the order of a few eV) so that the calculated spectra need to be uniformly shifted on the photon energy scale for comparison with the experimental data.

Fig. 1 displays the U M_4 HERFD-XAS spectra of UO_2, $NaUO_3$ and Pb_3UO_6. An improved energy resolution in comparison with conventional XAS allows one to clearly observe significant chemical shifts between the U M_4 lines of these compounds. UO_2 and Pb_3UO_6 contain nominal U(IV) and U(VI), respectively, therefore $NaUO_3$, whose U M_4 line appears in between those of UO_2 and Pb_3UO_6, is confirmed to have nominal U(V). The chemical shift between UO_2 and $NaUO_3$ is larger than between $NaUO_3$ and Pb_3UO_6 which can be explained by the proportionality between the shift and the change in the charge of the U atoms on going from one compound to another or by the change in the $5f$-shell occupancy (n_f). The calculations show that the difference in n_f is larger between UO_2 and $NaUO_3$ than between $NaUO_3$ and Pb_3UO_6 (see below) as could be expected from the experimental results. In addition, the improved resolution also allows us to state that $NaUO_3$ does not have any U(IV) fraction as claimed in Ref.[2] since the U(IV) signal is absent from the U M_4 spectrum of $NaUO_3$.

Besides an enhanced sensitivity to the changes in the chemical state of the actinide cation, the improved resolution makes the HERFD-XAS spectra sensitive to the strength of the $5f$ crystal-field interaction and crystal-field splittings in

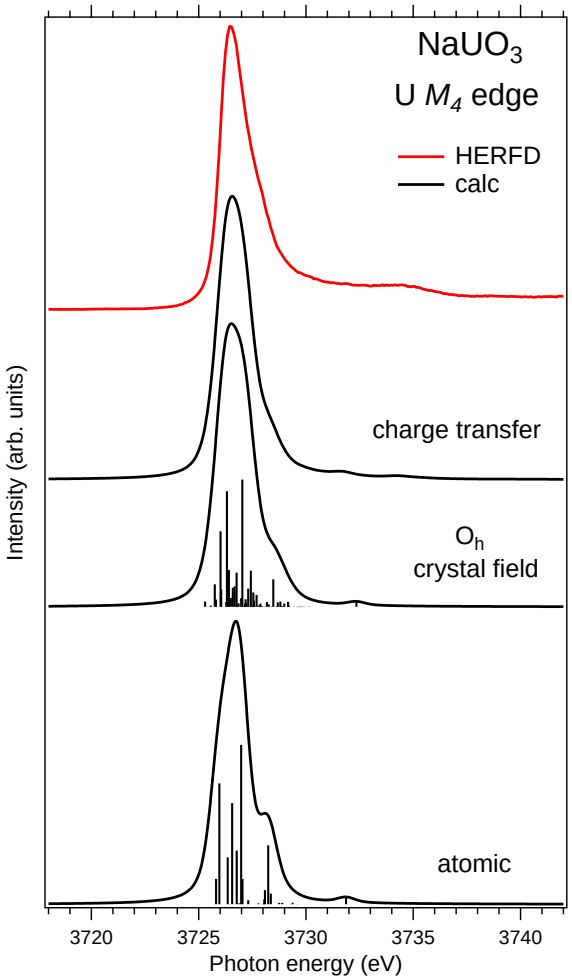

Figure 2. Experimental and calculated XAS spectra at the U M_4 edge of $NaUO_3$. The spectra were calculated using atomic and crystal-field multiplet theory for the U(V) ion and the Anderson impurity model, respectively.

the $5f$ shell. In Fig. 2, the U M_4 HERFD-XAS spectrum of $NaUO_3$ is compared to the results of atomic and crystal-field multiplet theory for the U(V) ion. The U cation in $NaUO_3$ is six-fold coordinated. The UO_6 octahedra are slightly distorted (with four U−O bonds a the length of 2.151(2) Å and the other two with a length of 2.142(1) Å [4]) and can be approximated by the O_h crystal-field symmetry. The XAS spectra at the U M_4 edge were calculated as transitions between the $3d^{10}5f^1$ (ground state) and $3d^9 5f^2$ (final state) electronic configurations using Slater integrals $F^k(5f, 5f)$, $F^k(3d, 5f)$ and $G^k(3d, 5f)$ reduced to 70% of their Hartree-Fock values (see the reasoning in Ref. [23]).

The atomic multiplet calculations for the $^2F_{5/2}$ ground state do not reproduce the shape of the experimental U M_4 spectrum very well. The calculated spectrum shows a hump on the low-energy side at ∼3725.8 eV which is not observed in the experiment, while the shoulder on the high-energy side at ∼3728.2 eV is too pronounced. The calculated spectral shape appears to be in better agreement with the experiment when the U(V) ion is placed in a cubic (O_h) crystal-field environment with six-fold coordination and using Wybourne's crystal-field parameters [24] for the $5f$ shell set to $B_0^4 = 2.03$ eV and $B_0^6 = 0.17$ eV. However, the calculated spectrum is somewhat too broad. In turn, taking the U $5f$−O $2p$ hybridization into account in the XAS calculations within the framework of AIM leads to a narrowing of the main U M_4 line and to the appearance of the so-called charge-transfer satellite at about 8 eV above the main line, i.e., at ∼3734.5 eV on the photon energy scale.

In the AIM calculations, the ground (final) state of the system was described using a linear combination of the $5f^1$ and $4f^2\underline{v}^1$ ($3d^9 5f^2$ and $3d^9 4f^3\underline{v}^1$) configurations where $\underline{v}$ stands for an electronic hole in the O $2p$ band. In the limit of the U $5f$−O $2p$ hybridization term $V \to 0$, the difference between the configuration averaged energies for the ground state can be written as $E(5f^2\underline{v}^1) - E(5f^1) = \Delta$ (where $\Delta \equiv \epsilon_f - \epsilon_n$, with ϵ_n corresponding to the center of the O $2p$ band) which is the so-called charge-transfer energy (ϵ_f and ϵ_n are one-electron energies of the U $5f$ and O $2p$ levels). For the final state, this difference is $E(3d^9 5f^3\underline{v}^1) - E(3d^9 5f^2) = \Delta + U_{ff} - U_{fc}$, where U_{ff} denotes the $5f$-$5f$ Coulomb interaction and U_{fc} is the $3d$ core hole potential acting on the $5f$ electron. Treated as parameters, the Δ, U_{ff} and U_{fc} values were taken to be 4.0, 3.5 and 6.0 eV, respectively.

The hybridization term (hopping matrix element) between $5f^1$ and $5f^2\underline{v}^1$ configurations in the ground state was taken as $V_g = 1.2$ eV. To account for the electronic-configuration dependence of V, this value was scaled down to 75% ($0.75V_g$=V_m) to describe the mixing between $3d^9 5f^2$ and $3d^9 5f^3\underline{v}^1$ configurations in the final state. [16,25] The $3d_{3/2}$ core-hole-lifetime Lorentzian broadenings (Γ_m) was taken as 0.35 eV with an additional Gaussian convolution to account for the instrumental resolution.

The U M_4 HERFD-XAS spectrum of $NaUO_3$ exhibits the structure on the high-energy side at ∼3734.5 eV which is reproduced as a charge-transfer satellite due to U $5f$−O $2p$ hybridization in the AIM calculations. The contributions of the $5f^1$ and $4f^2\underline{v}^1$ configuration in the ground state were estimated to be 68% and 32%, respectively, thus resulting in $n_f = 1.32$ electrons. Such a n_f value indicates a significant covalent character for $NaUO_3$ and the estimated values of Δ and U_{ff} and their ratio suggest that $NaUO_3$ is not a Mott-Hubbard system by contrast with UO_2.

Since the U M_4 HERFD-XAS spectrum is a result of the varying cross-section of core-to-core RIXS [9,11] upon sweeping the incident photon energy throughout the M_4 edge, we calculated the RIXS map around the U $M\beta$ line to take the corresponding cut and compare it with the conventional XAS spectrum. To simplify the computational framework, this comparison was made for the U(V) ion in the cubic (six-fold ligand coordination) crystal-field environment, while the effects of U$5f$−O $2p$ hybridizations which lead to the appearance of low-intense high-energy satellite were omitted.

The RIXS map was calculated with equation 1 for the path $3d^{10}5f^1 \to 3d^9 5f^2 \to 4f^{13}5f^2$ with Γ_m and Γ_j set to 1.65 eV and 0.35 eV, respectively. To take the experimental geometry into account, the incident photons had linear polarization along the z-axis so that $q_1 = 0$. For the scattering angle of 90° and the incident photon polarization in the scattering plane, the spectral intensity was expressed [26] as $I_{q_2,q_1} = (I_{1,0} + I_{-1,0})$.

Figs. 3a and 3b show the calculated RIXS map around the U $M\beta$ line and comparison of the corresponding cut of this map (to represent the HERFD-XAS scan) with the calculated conventional U M_4 XAS spectrum for the U(V) ion in the cubic crystal-field environment, respectively. The result of the map cut is a one-dimensional spectrum of intensity I versus incident energy ω obtained for fixed emitted energy

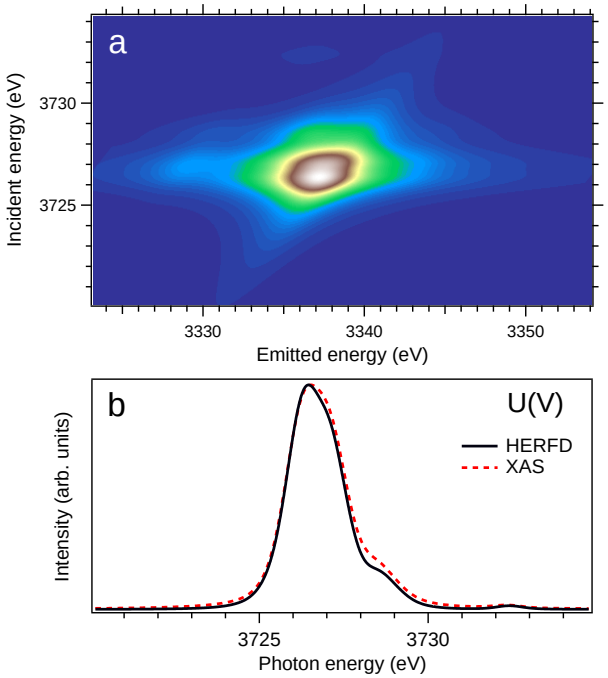

Figure 3. Calculated a) RIXS map around the $M\beta$ line of the U(V) ion in the cubic crystal field environment, b) HERFD-XAS and conventional XAS spectra at the U(V) M_4 edge.

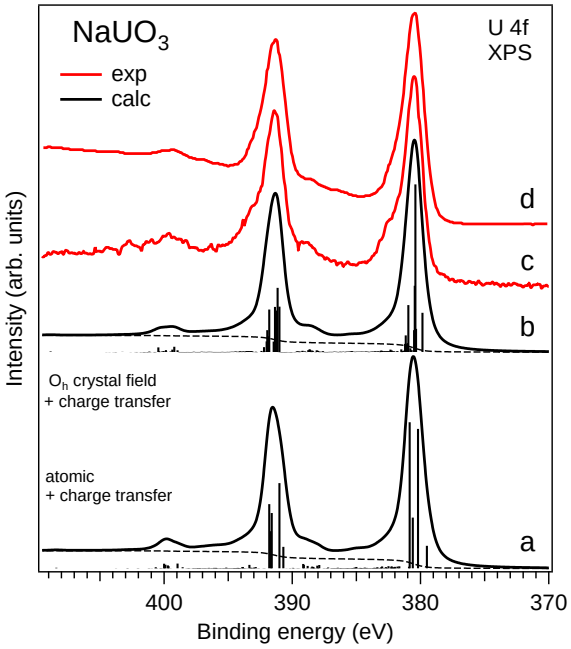

Figure 4. Calculated U $4f$ XPS spectra of the U(V) system using the Anderson impurity model: a) without taking the crystal-field interaction in the $5f$ shell into account (curve *a*); b) when including the cubic crystal field (curve *b*). The spectra are compared with the experimental data from Ref.[27] (curve *c*) and Ref.[7] (curve *d*). Curve *c* was shifted to match the energy scale of curve *d*. The dashed curves represent the photoelectron background.

ω' corresponding to the main maximum of the $4f_{5/2} \rightarrow 3d_{3/2}$ line. The comparison reveals only small differences between the calculated conventional XAS and HERFD-XAS spectra, thus justifying the use of HERFD-XAS at the M edges of the actinides as the high-resolution XAS-replacement via a reduction of the core-hole lifetime broadening.

The results of our estimations of the AIM parameters for $NaUO_3$ from the analysis of the HERFD-XAS data at the U $3d$ edge are also supported by the calculations of the U $4f$ XPS spectrum (Fig. 4). The experimental data[7,27] were well reproduced using the same set of AIM parameters apart from that for U_{fc} which is expected to be smaller for the $4f$ level. The U_{fc} value was set to 5.0 eV. In this case, the final state configurations with the $4f$ core hole had the same number of $5f$ electrons as the corresponding ground state configurations due to the ionization process and excited electron leaving the system. The U_{fc} value is similar to that used in the AIM calculations[28] of the U $4f$ XPS data of UO_2.

In Fig. 4, two simulated U $4f$ XPS spectra (curves *a* and *b*) are displayed which were calculated for the U(V) system in the framework of AIM when taking the multiplet due to intra-atomic interactions at the U site into account. In the calculations of spectrum *a*, the crystal-field interaction for the $5f$ shell was not included, while spectrum *b* was calculated taking the O_h crystal field effects into account. Both calculated spectra reproduce the experimental data in terms of the energy separation (~8 eV) and relative intensity of the charge-transfer satellites at binding energies of ~388.5 and ~399.5 eV for the main U $4f_{7/2}$ and $4f_{5/2}$ lines, respectively. When considering the cubic crystal field environment for the U(V) ion with $B_0^4 = 2.03$ eV and $B_0^6 = 0.17$ eV, the asymmetry on the low binding energy side of the main $4f_{7/2}$ and $4f_{5/2}$ lines are removed, and the calculated line shape is in better agreement with the experiment. This indicates that XPS spectra are sensitive to the crystal-field splittings in the $5f$ shell even if the latter effects are more pronounced in the HERFD-XAS spectra.

The crystal-field parameter values $B_0^4 = 2.03$ eV and $B_0^6 = 0.17$ eV are in agreement with those derived from the optical absorption spectroscopy experiment.[29–31] Table 1 compares the lowest excited states of the U $5f$ multiplet obtained in the AIM calculations with those measured by optical absorption spectroscopy. The agreement between theory and experiment is rather good. The inclusion of the U $5f$–O $2p$ hybridization in the calculations allowed to improve the results in terms of agreement with experimental values.

Table 1. Lowest states of the U $5f$ multiplet (in meV) calculated for the cubic crystal-field environment (with and without the U $5f$-O $2p$ hybridization) within the Anderson impurity model and comparison with the results obtained by optical absorption spectroscopy.[29,30]

State	Exp.	Calculations (no hybridization)	Calculations
Γ_7		0	0
Γ_8	561	538	515
Γ_7'	883	1040	989
Γ_8'	1282	1551	1484
Γ_6	1616	1848	1770

In the orthorhombic structure of Pb_3UO_6,[14] where uranium is in oxidation state U(VI), the UO_6 octahedra are distorted with the apex oxygen atoms at a slightly greater distance (2.167(9) Å and 2.214(9) Å, respectively) from the central uranium than the other four in the equatorial plane (2.040(11) Å, 2.060(11) Å, 2.049(11) Å, 1.991(11) Å, respectively). Although, one would expect for the U(VI) system the main line of the M_4 edge to be a single peak as reported for the uranyl U(VI) groups,[9,11] the main U M_4 XAS line of Pb_3UO_6 reveals some splittings as shown in Fig. 5.

As for $NaUO_3$, the U M_4 HERFD-XAS spectrum of

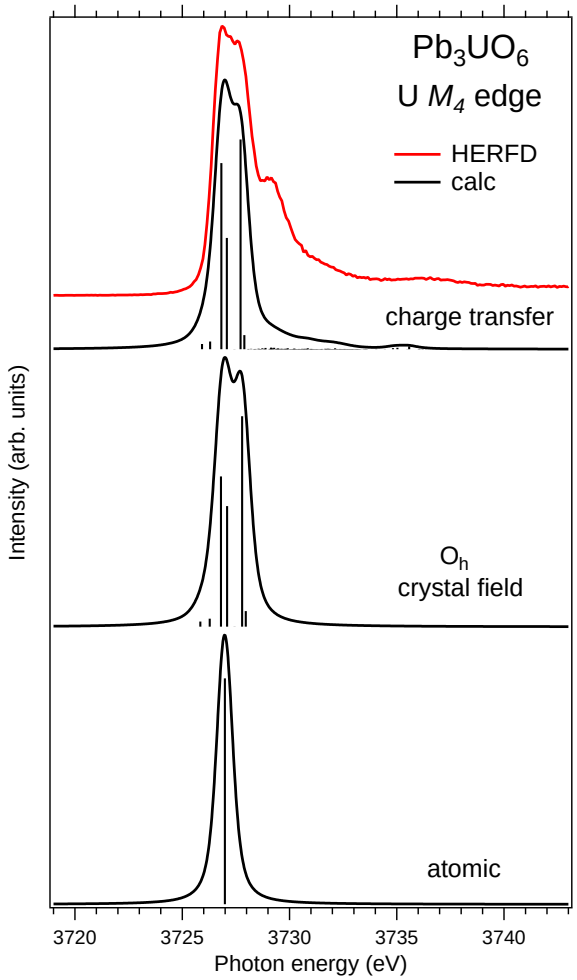

Figure 5. Experimental and calculated XAS spectra at the U M_4 edge of Pb_3UO_6. The spectra are calculated using atomic and crystal-field multiplet theory for the U(VI) ion and the Anderson impurity model, respectively.

Pb_3UO_6 is compared to the results of the atomic-, crystal-field multiplet (in the O_h approximation) and AIM calculations for the U(VI) system. The spectra were calculated for transitions between the $5f^0$ and $3d^95f^1$ configurations when using the atomic- and crystal-field multiplet theory, respectively. The atomic multiplet calculations for the transitions between the $5f^0$ and $3d^95f^1$ configurations in the $^1S_0$ ground state produced only one multiplet pole (Fig. 5), while the cubic (O_h) crystal-field environment of the U(VI) ion caused the splitting of the main U M_4 XAS line due to splittings of the states of the $3d^95f^1$ configuration. The gain in resolution allows to probe the crystal-field interactions in the $5f$ shell and to extract information on the crystal-field effects directly from the XAS data in the manner commonly used for the $L_{2,3}$ edges of $3d$ transition metal systems.

The U $5f-$O $2p$ hybridization and covalency effects are expected to be significant in the case of the U(VI) system. For this reason, in the AIM calculations for Pb_3UO_6, the ground state was described as a combination of the $5f^0$, $5f^1\underline{v}^1$ and $5f^2\underline{v}^2$ configurations, while the final state of the XAS process was described as a mixture of the $3d^95f^1$, $3d^95f^2\underline{v}^1$ and $3d^95f^3\underline{v}^2$ configurations. The model parameters had the following values: $\Delta = 2.0$ eV, $U_{ff} = 3.0$ eV, $U_{fc} = 5.0$ eV, $V_g = 1.2$ eV and $V_m = 0.9$ eV.

In the limit of $V \to 0$, the difference between the configuration averaged energies for the ground state in our AIM calculations was $E(5f^1\underline{v}^1) - E(5f^0) = \Delta = 2.0$ eV and $E(5f^2\underline{v}^2) - E(5f^1\underline{v}^1) = \Delta + U_{ff} = 5.0$ eV. For the final state it was $E(3d^95f^2\underline{v}^1) - E(3d^95f^1) = \Delta + U_{ff} - U_{fc} = 0.0$ eV and $E(3d^95f^3\underline{v}^2) - E(3d^95f^2\underline{v}^1) = \Delta + 2U_{ff} - U_{fc} = 3.0$ eV. The Slater integrals were scaled down to 80% of their Hartree-Fock calculated values. The crystal field parameters for the U $5f$ shell were set to $B_0^4 = 2.03$ eV and $B_0^6 = 0.80$ eV. Γ_m was set to 0.35 eV and an additional Gaussian broadening was applied to match the experimental resolution.

In these AIM calculations, taking the the U $5f-$O $2p$ hybridization into account led to the appearance of additional transitions on the high-energy side of the calculated XAS spectrum (Fig. 5) as compared to the crystal-field multiplet theory. This improved the agreement with the experimental data, though the structure at ~3729.2 eV was not well reproduced. The results of the present calculations indicate that the structure observed in the U M_4 HERFD-XAS spectrum of Pb_3UO_6 in the energy range between ~3735.0 and ~3738.5 eV can be assigned to a U $5f-$O $2p$ charge-transfer satellite. Our calculations also suggest that the contributions of the $4f^0$, $4f^1\underline{v}^1$ and $4f^2\underline{v}^2$ configurations in the ground state of Pb_3UO_6 amount to 32%, 52% and 16%, respectively, thus resulting in $5f$ occupancy $n_f = 0.84$. The 3729.2-eV structure might be associated with the U bonds to apex oxygen due to somewhat different U $5f-$O $2p$ charge-transfer energy and hybridization strength as compared to bonds in the equatorial plane.

The comparison of the n_f values for UO_2, $NaUO_3$ and Pb_3UO_6 which were estimated from AIM as 2.22 (Refs.[11,28,32]), 1.32 and 0.84 electrons in the ground state, respectively, shows that the difference in $5f$ occupancy is larger between UO_2 and $NaUO_3$ than between $NaUO_3$ and Pb_3UO_6. This justifies the observed larger chemical shift between the U M_4 HERFD-XAS spectra of UO_2 and $NaUO_3$ (U(IV) and U(V) systems) compared to the shift between $NaUO_3$ and Pb_3UO_6 (U(V) and U(VI) systems), though the final value of the shift can be affected by other factors, such as e.g. local symmetry around the U atom and induced splittings in the $5f$ shell.

In conclusion, the higher resolution of the HERFD mode of XAS at the actinide $3d$ edge allows to resolve the crystal-field split states, to determine the strength of crystal-field interactions in the $5f$ shell, and to detect local symmetry changes in the actinide compounds. We were able to observe for the first time the crystal-field $5f$ splittings of complex uranates directly from their XAS spectra and determine the corresponding crystal field parameters. The derived values indicate that the crystal-field is strong for the structures of the studied uranates. Furthermore, the AIM analysis of the newly-acquired high-resolution HERFD-XAS data, including the energy separation of charge-transfer satellites from the main line, allowed us to estimate the $5f$ occupancy and covalency effects which indicate significant U $5f-$O $2p$ hybridization and a marked covalent character for these uranate U(V) and U(VI) systems.

References

(1) C. Miyake, H. Sakurai, S. Imoto, *Chem. Phys. Lett.* **1975**, *36*, 158-160.
(2) G. C. Allen, N. R. Holmes, *Can. J. Appl. Spectros.* **1993**, *38*, 124-130.
(3) A. M. Chippindale, P. G. Dickens, W. T. A. Harrison, *J. Solid State Chem.* **1989**, *78*, 256-261.
(4) S. Van den Berghe, A. Leenaers, C. Ritter, *J. Solid State Chem.* **2004**, *177*, 2231-2236.

(5) A. V. Soldatov, D. Lamoen, M. J. Konstantinović, S. Van den Berghe, A. C. Scheinost, M. Verwerft, *J. Solid State Chem.* **2007**, *180*, 54-61.
(6) A. L. Smith, P. E. Raison, L. Martel, T. Charpentier, I. Farnan, D. Prieur, C. Hennig, A. C. Scheinost, R. J. M. Konings, A. K. Cheetham, *Inorg. Chem.* **2014**, *53*, 375-382.
(7) J.-H. Liu, S. Van den Berghe, J. Konstantinović, *J. Solid State Chem.* **2009**, *182*, 1105-1108.
(8) K. O. Kvashnina, Y. O. Kvashnin, J. R. Vegelius, A. Bosak, P. M. Martin, S. M. Butorin, *Anal. Chem.* **2015**, *87*, 8772-8780.
(9) K. O. Kvashnina, Y. O. Kvashnin, S. M. Butorin, *J. Electron Spectros. Rel. Phenom.* **2014**, *194*, 27-36.
(10) S. M. Butorin, A. Modin, J. R. Vegelius, M.-T. Suzuki, P. M. Oppeneer, D. A. Andersson, D. K. Shuh, Local Symmetry Effects in Actinide 4*f* X-ray Absorption in Oxides. Accepted for publication in *Anal. Chem.* DOI: 10.1021/acs.analchem.5b04380.
(11) K. O. Kvashnina, S. M. Butorin, P. Martin, P. Glatzel, *Phys. Rev. Lett.* **2013**, *111*, 253002.
(12) C. Gauthier, V. A. Sole, R. Signorato, J. Goulon, E. Moguiline, *J. Synchrotron Radiat.* **1999**, *6*, 164-166.
(13) P. Glatzel, U. Bergmann, *Coordin. Chem. Rev.* **2005**, *249*, 65-95.
(14) M. Sterns, J. B. Parise, C. J. Howard, *Acta Cryst. C* **1986**, *42*, 1275-1277.
(15) P.W. Anderson, *Phys. Rev. B* **1961**, *124*, 41.
(16) S. M. Butorin, D. C. Mancini, J.-H. Guo, N. Wassdahl, J. Nordgren, M. Nakazawa, S. Tanaka, T. Uozumi, A. Kotani, Y. Ma, K. E. Myano, B. A. Karlin, and D. K. Shuh, *Phys. Rev. Lett.* **1996**, *77*, 574.
(17) M. Nakazawa, H. Ogasawara, A. Kotani, *Surf. Rev. Lett.* **2002**, *9*, 1149-1153.
(18) H. Ogasawara, A. Kotani, R. Potze, G. A. Sawatzky, B.T. Thole, *Phys. Rev. B* **1991**, *44*, 5465-5469.
(19) J. C. Slater, *Phys. Rev.* **1929**, *34*, 1293.
(20) R. D. Cowan, *Theory of Atomic Structure and Spectra* (University of California Press, Berkeley, 1981).
(21) P. H. Butler, *Point Group Symmetry Applications: Methods and Tables* (Plenum Press, New York, 1981).
(22) B. T. Thole, G. van der Laan, P. H. Butler, *Chem. Phys. Lett.* **1988**, *149*, 295.
(23) J. Sugar, *Phys. Rev. B* **1972**, *5*, 1785-1792.
(24) B. G. Wybourne, *Spectroscopic Properties of Rare Earths*, Wiley, New York, 1963.
(25) O. Gunnarsson, O. Jepsen, *Phys. Rev. B* **1988**, *38*, 3568.
(26) M. Nakazawa, H. Ogasawara, A. Kotani, *J. Phys. Soc. Jpn* **2000**, *69*, 4071-4077.
(27) E. Simons, *XPS-Studie Van De Uraniumvalentie in Alkalimetaal-Uranaten.* Hogeschool Antwerpen (Antwerpen), 2000.
(28) T. Yamazaki, A. Kotani, *J. Phys. Soc. Jpn* **1991**, *60*, 49-52.
(29) S. Kemmler-Sack, *Z. Anorg. Allg. Chem.* **1968**, *363*, 295-304.
(30) B. Kanellakopulos, E. Henrich, C. Keller, F. Baumgärtner, E. König, V.P. Desai, *Chem. Phys.* **1980**, *53*, 197-213.
(31) Y. Hinatsu, *J. Alloys & Comp.* **1994**, *203*, 251-257.
(32) S. M. Butorin, unpublished results.